International Journal of Bifurcation and Chaos, Vol. 16, No. 5 (2006) 1537–1546
© World Scientific Publishing Company

SPATIOTEMPORAL PATTERN FORMATION ON THE ACE16k CNN CHIP

M. E. YALÇIN*
Faculty of Electrical and Electronic Engineering,
Istanbul Technical University,
80626, Maslak, İstanbul, Turkey
mustak.yalcin@itu.edu.tr

J. A. K. SUYKENS
Department of Electrical Engineering, ESAT-SCD-SISTA,
Katholieke Universiteit Leuven,
Kasteelpark Arenberg 10, B-3001 Leuven (Heverlee), Belgium
johan.suykens@esat.kuleuven.ac.be

Received May 16, 2005; Revised July 7, 2005

In this paper, we report on pattern formation occurring on the ACE16k CNN chip. The CNN chip can be programmed with a cloning template in order to generate spiral waves and autowaves. The waves diffract from *internal sources* which cannot be relocated on the network. However, by using initial and/or input images, sources (*external sources*) can be located at any place on the network. Furthermore a competition between autowaves generated by external and internal sources is observed. Propagation of autowaves on the inhomogeneous CNN array, formed by the fixed-state map, is presented.

Keywords: Cellular neural networks; CNN-UM; spatiotemporal pattern formation; autowaves; spiral waves.

1. Introduction

Autowaves are a particular class of waves resulting from strongly nonlinear active media [Munuzuri *et al.*, 1995]. The fundamental properties of autowaves are

- the shape and amplitude of autowaves remain constant during the propagation,
- they do not reflect at the medium boundaries,
- two colliding autowaves annihilate.

The CNN framework provides a very useful methodology for studying spatial-temporal pattern formation [Chua, 1998; Manganaro *et al.*, 1999; Chua *et al.*, 1995]. Autowaves are well described by reaction–diffusion equations. As a result the reaction–diffusion CNN model has been widely used for generating such waves. In [Munuzuri *et al.*, 1995] a review on the study of spatial-temporal behavior on an array of Chua's circuits, where Chua's circuit is used as the reaction term in the model, has been presented. Manganaro *et al.* [1999] have used a second-order system for the reaction term and have observed autowaves, spiral waves and Turing patterns. In fact, the model used by Manganaro *et al.* [1999] can be thought of as a two layer CNN with a Chua–Yang model. In [Carmona *et al.*, 2003] spatial-temporal phenomena on CNNs have been experimentally verified for a two layer CNN. The CACE1k (Complex Analogic Cellular Engine) chip [Carmona *et al.*, 2003] is a VLSI

*Author for correspondence.

implementation of the two layer CNN. This prototype chip contains 32×32 identical cells, surrounded by the boundary conditions of the CNN dynamics. In fact CACE1k is a two-layer Analogic Cellular Engine (ACE) chip which is designed based on CNN-Universal Machine (CNN-UM) architecture [Roska & Chua, 1993]. ACE chips contain an array of identical cells on a single layer and they are also designed based on the CNN-UM architecture. In this paper, experimental observations of spatiotemporal pattern phenomena on an ACE16k (which has an array of 128×128 cells) chip are shown. The first experimental observation of these phenomena on a ACE16k chip has been reported by Yalçın *et al.* in [Yalçın *et al.*, 2004] and [Yalçın *et al.*, 2005].

This paper is organized as follows. Section 2 briefly describes a number of elements of ACE16k chip which are relevant to this paper. Section 3 presents pattern formation on an ACE16k chip. Section 4 reports propagation of autowaves on an inhomogeneous CNN array formed by the fixed-state map.

2. ACE16 CNN Chip

Analogic Cellular Engines (ACEs) are designed based on the CNN-Universal Machine (CNN-UM) architecture. They are capable of realizing a very large variety of image related spatial-temporal operations and algorithms through the execution of a suitable sequence of instructions (or templates). The ACE16k chip is the third generation of ACE chips and it consists of an array of 128×128 identical analog Full-range CNN cells. Complex dynamic behaviors in the Full-range model have been studied in [Biey *et al.*, 2002]. A strange attractor similar to the chaotic attractor observed in a CNN with Chua–Yang model has been observed.

Unfortunately, precise modeling of a single cell in the ACE16k CNN chip, which has approximately 180 transistors per cell, is a difficult task. The ACE16k chip has eight functional blocks. However, cell $\mathfrak{C}_{i,j}$ $(i,j = 1,2,\ldots,128)$ dynamics in ACE16k are basically defined by two functional blocks which are multipliers and processing blocks [Linan *et al.*, 2002]. The multipliers are implementing the synaptic law of the model given by

$$I^s_{i,j} = \sum_{k,l\in\mathcal{S}_{i,j}(1)} a_{k-i,l-j}x_{1_{k,l}} \tag{1}$$

with sphere of influence $\mathcal{S}_{i,j}(1)$, where [Chua, 1998]

$$\mathcal{S}_{i,j}(1) = \{\mathfrak{C}_{k,l} : \max(|k-i|,|l-k|) \le 1,\ 1 \le k \le 128,\ 1 \le l \le 128, k \ne i, l \ne j\} \tag{2}$$

and $a_{k,l}, x_{1_{i,j}} \in \mathbb{R}$. The processing block implements the essential function of ACE16k. The synaptic input $I^s_{i,j}$ is the input of the processing block and its output is a nonlinear function $g(\cdot)$. It has three variables $x_1, x_2, x_3 \in \mathbb{R}$ which can be either programmed as the state variable $x \in \mathbb{R}$ or as an input $u \in \mathbb{R}$ of the cell $\mathfrak{C}_{i,j}$ (via the switches in the ACE16k chip). The processing block also has a constant threshold $z \in \mathbb{R}$. The cell dynamics of ACE16k are described by the following mathematical model

$$\dot{x}_{i,j} = -g(x_{i,j}) + 2ax_{1_{i,j}} + 2bx_{2_{i,j}} + 2cx_{3_{i,j}} + 2z_{i,j} + I^s_{i,j}. \tag{3}$$

where a, b, $c \in \mathbb{R}$. The execution mode corresponds to the dynamics obtained after the switches are configured. Ten execution modes have been defined for ACE16k in the Aladdin system [Aladdin, 2003] which is a professional CNN chip prototyping system (CCPS), interfacing the ACE16k CNN chip to digital systems [Roska *et al.*, 1999]. Table 1 shows which of the x_1, x_2, x_3 variables can be set to the state variable or the input for a given execution mode. As an example, the cell dynamics of ACE16k for execution mode 9 are given by

$$\begin{aligned} \dot{x}_{i,j} &= -g(x_{i,j}) + 2au_{i,j} + 2bx_{i,j} + 2cx_{i,j} + I^s_{i,j} \\ I^s_{i,j} &= \sum_{k,l\in\mathcal{S}_{i,j}(1)} a_{k-i,l-j}u_{k,l}. \end{aligned} \tag{4}$$

The cloning template structures are also defined by the chosen execution mode such that mode 1 only allows the following cloning template structure

$$A = \begin{bmatrix} a_{-1,-1} & a_{-1,0} & a_{-1,1} \\ a_{0,-1} & 2a_{0,0} & a_{0,1} \\ a_{1,1} & a_{1,0} & a_{1,1} \end{bmatrix}, \quad B = \begin{bmatrix} 0 & 0 & 0 \\ 0 & 2b_{0,0} & 0 \\ 0 & 0 & 0 \end{bmatrix}, \quad z = 0. \tag{5}$$

The fixed-state map of a CNN is a binary image. It specifies which CNN cells are in a certain

Table 1. Execution mode for the ACE16k CNN chip and corresponding configuration for the variables.

Mode	Variables Configurations
1	$x = x_1$ $x_2 = u$ $z = 0$
2	$x = x_1$ $x_2 = u$
3	$x = x_2$ $x_1 = u$ $z = 0$
4	$x = x_2$ $x_1 = u$
5	$x = x_2$ $x_1 = x_3 = u$ $z = 0$
6	$x = x_1 = x_2$ $x_3 = 0$ $z = 0$
7	$x = x_1 = x_2$ $x_1 = 0$
8	$x = x_1 = x_2$ $x_3 = u$
9	$x = x_2 = x_3$ $x_1 = u$ $z = 0$
10	$x = x_1 = x_2 = x_3$ $z = 0$

active or inactive state for all time. The state variables of these cells are frozen to fixed values and do not change in time. In Fig. 1 the frozen cells are shown with a black square. The corresponding

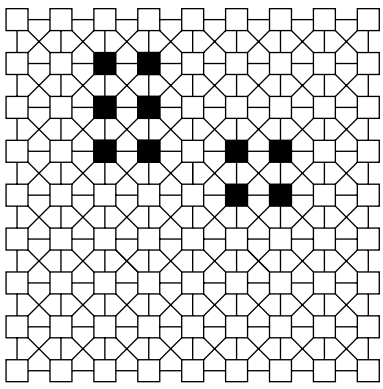

Fig. 1. Active and frozen cells on a CNN array. The black squares represent frozen cells when the fixed-state map Eq. (6) is chosen.

fixed-state map for Fig. 1 is given by

$$M = \begin{bmatrix} 0 & 0 & 0 & 0 & 0 & 0 & 0 & 0 & 0 \\ 0 & 0 & 1 & 1 & 0 & 0 & 0 & 0 & 0 \\ 0 & 0 & 1 & 1 & 0 & 0 & 0 & 0 & 0 \\ 0 & 0 & 1 & 1 & 0 & 1 & 1 & 0 & 0 \\ 0 & 0 & 0 & 0 & 0 & 1 & 1 & 0 & 0 \\ 0 & 0 & 0 & 0 & 0 & 0 & 0 & 0 & 0 \\ 0 & 0 & 0 & 0 & 0 & 0 & 0 & 0 & 0 \\ 0 & 0 & 0 & 0 & 0 & 0 & 0 & 0 & 0 \\ 0 & 0 & 0 & 0 & 0 & 0 & 0 & 0 & 0 \end{bmatrix}. \quad (6)$$

The fixed state option offers implementing an inhomogeneous structure for the CNN array and the ACE16k CNN chips. In VLSI implementations of ACE16k, a given fixed-state map is realized via the x_3 variable [Aladdin, 2003]. For further information about the ACE16k chip, we refer to [Rodriguez-Vazquez *et al.*, 2004] and [Linan *et al.*, 2002].

3. Experiments

For the discussed experiments, the vector of the recommended settings of the internal references (<hwparams>) is set to [0 0 0 229 200 172 145 109 78 37 23] [Aladdin, 2003]. The internal references include optical, weight and signal references which are setting currents and voltages for the specific blocks in the ACE16k. The current and bias that are defining the threshold z are set to 0. Furthermore, a fixed boundary condition with value 0 was used during our experiments.

3.1. *Experimental results: Autowaves*

In a first experiment, the following templates

$$A = \begin{bmatrix} 0 & 0 & 0 \\ 0 & -3 & 0 \\ 0 & 0 & 0 \end{bmatrix}, \quad B = \begin{bmatrix} 0 & 0 & 0 \\ 0 & -3 & 0 \\ 0 & 0 & 0 \end{bmatrix} \quad (7)$$

were chosen with execution mode 1 and a full white image was used as initial state and input. Fig. 2 shows three consecutive snapshots depicting the obtained autowave during the time evolution for the cloning template Eq. (7). Four wave sources shown in Fig. 2(a) which are located at the corners have been observed. They are called *internal sources* because these sources stay active during the different experiments. The waves in Fig. 2(a) show the fundamental properties of autowaves: two waves that are spreading in opposite directions do not pass each other but mutually annihilate. The



(a) (b) (c)

Fig. 2. (a)–(c) Time evolution for the cloning template Eq. (7). The waves are diffracting from the corners. The shape and amplitude of the waves remain constant during propagation. There is no interference between waves and the colliding waves annihilate. Furthermore, the waves do not reflect from the boundaries of the network.

shape and amplitude of the waves remain constant during propagation and the waves do not reflect at the boundaries of the network.

In a second experiment, it is shown that new autowave sources, called here *external sources*, can be imposed at any place on the network. A source can be located with black dots on the initial and input images. In Fig. 3(a) (the box around the figure is not a part of the image) a source is located on the left-bottom corner. Two consecutive snapshots depict the resulting autowave in time. One can clearly distinguish two autowave sources in Fig. 3(b): the *internal source* of the network and the source positioned at the black dot on the initial and input images. This experiment has also been repeated in the case of four sources placed at the corners [see Fig. 4(a)]. The result is shown in Fig. 4(b) and a consecutive frame is shown in Fig. 4(c). Figures 4(b) and 4(c) clearly show that the waves diffract from the defined sources. They interact in the middle of the network and then annihilate each other.

Figure 5 shows the competition [Munuzuri *et al.*, 1995] between the autowaves generated by four internal sources and one external source. Initially the waves from the external and internal sources start interacting and then annihilate [see Fig. 5(a)]. The region where they interact and annihilate is drifting towards the top-right corner of the network. Figures 5(a)–5(f) successively show snapshots on the network during the competition. A movie file for whole time evolution can be seen in http://www.esat.kuleuven.ac.be/sista/chaoslab/autowaves/test2.avi.



(a) (b) (c)

Fig. 3. (a) Image taken as initial and input image (the box around the figure is not a part of the image). (b)–(c) Evolution in time for the cloning template Eq. (7) corresponding to the initial and input images from (a).

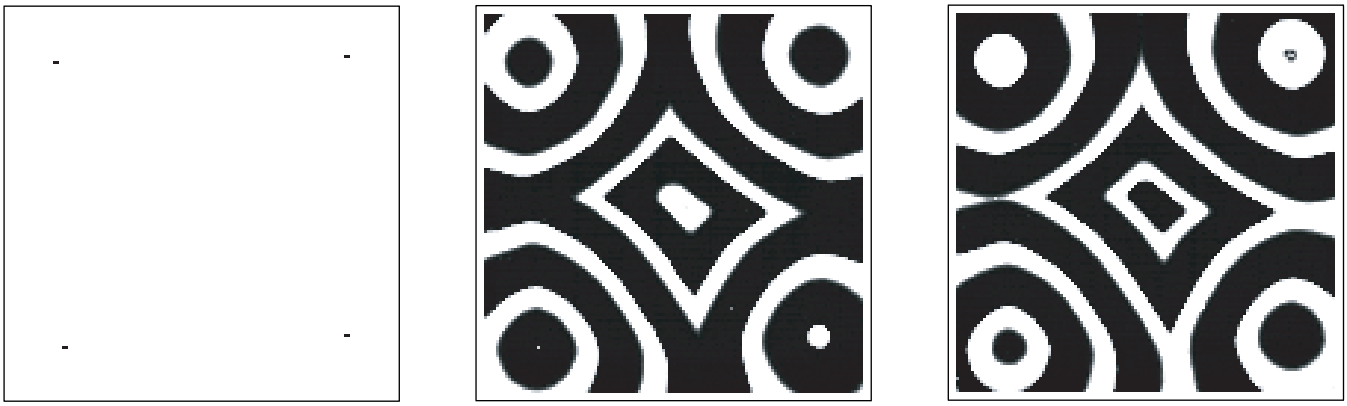

(a) (b) (c)

Fig. 4. (a) Initial and input image. (b)–(c) Evolution in time for the cloning template Eq. (7) corresponding to the initial and input images from (a).

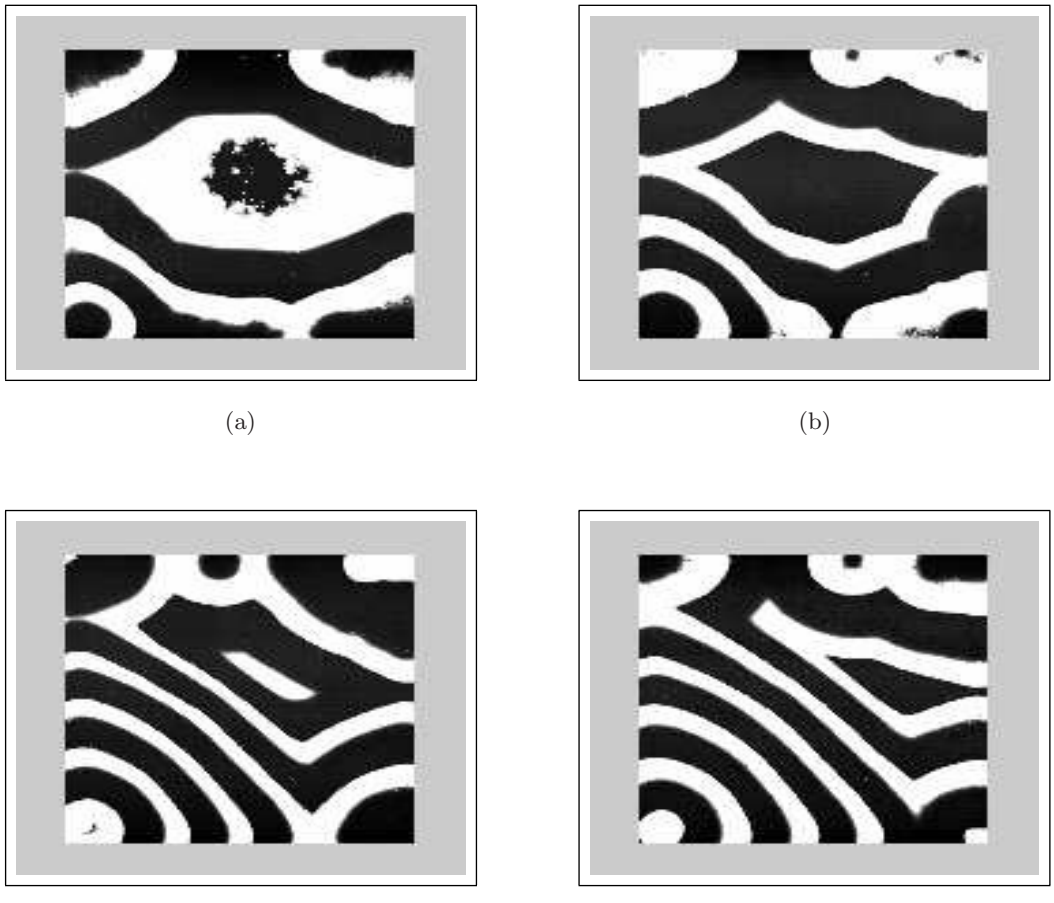

(a) (b)

(c) (d)

Fig. 5. Competition between autowaves resulting from the chip-internal sources and an autowave resulting from an externally imposed source. The interaction region of the autowaves moves to the top-right corner of the network.

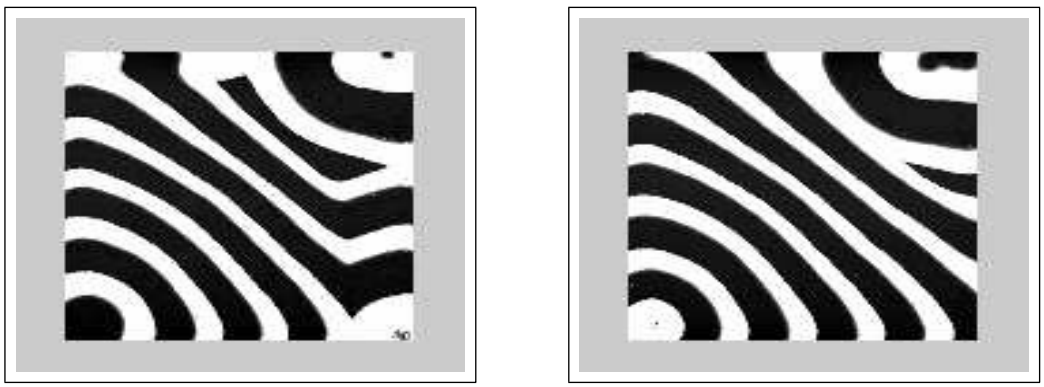

(e) (f)

Fig. 5. (*Continued*)

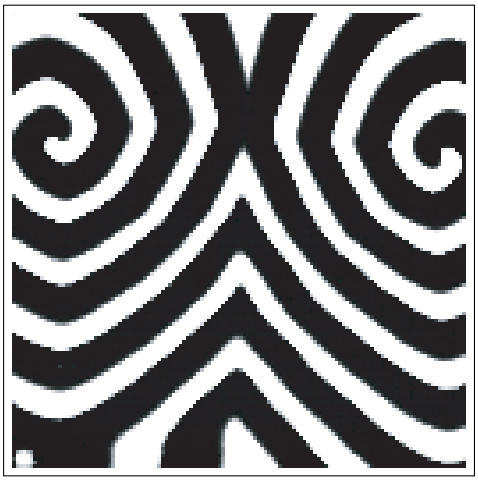

Fig. 6. Spiral wave obtained on the ACE16k chip for a full white image as initial image.

3.2. *Experimental results: Spiral waves*

In a next experiment, we use the following templates with execution mode 1

$$A = \begin{bmatrix} 0 & 0 & 0 \\ 0 & -3 & 0 \\ 0 & 0 & 0 \end{bmatrix}, \quad B = \begin{bmatrix} 0 & 0 & 0 \\ 0 & 0 & 0 \\ 0 & 0 & 0 \end{bmatrix} \tag{8}$$

which has the same feedback template as the previous experiment. However, it includes a zero central element in the control template. Figure 6 shows the obtained result with a full white image as initial condition.

The network has two internal spiral wave sources at the left- and right-hand sides of the image.

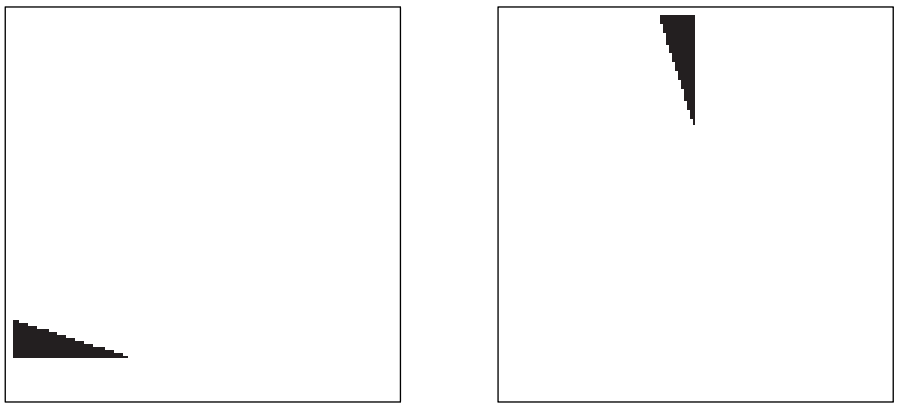

(a) (b)

Fig. 7. (a) and (b) Two different initial images. (c) and (d) Spiral waves obtained for the initial states (a) and (b), respectively.

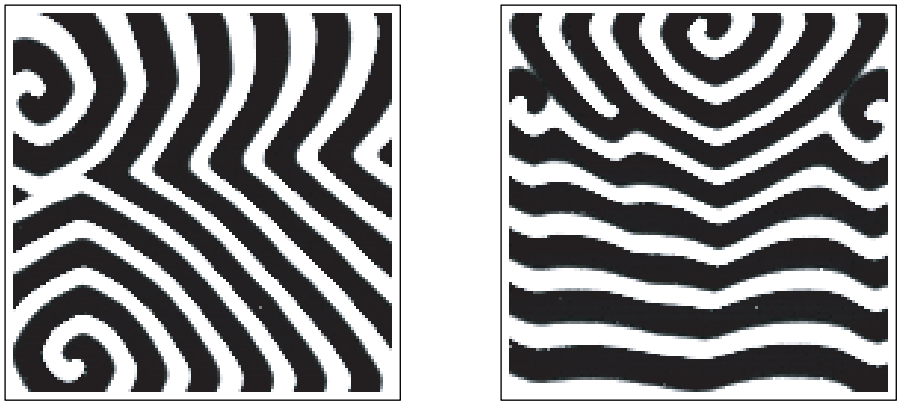

(c) (d)

Fig. 7. (*Continued*)

Using the given initial conditions in Figs. 7(a) and 7(b), external sources for spiral wave can be located on the network as shown in Figs. 7(c) and 7(d).

4. Propagation of Autowaves on the Inhomogeneous CNN Arrays

In this first experiment, the network has been divided into two sub-networks using the fixed-state given in Fig. 8(c). In order to see the propagation of autowaves on these two subnetworks, Fig. 8(a) has been chosen as initial and input image and template Eq. (7) has been used. As expected, one external autowave source is located on each subnetwork. There is no interference between the autowaves propagating from external sources because of the isolation by the fixed-state [see Fig. 8(c)]. However, there is an interaction between the waves propagated from the external source and the internal sources on the same subnetwork at the right-hand side of the network.

In a second experiment, Fig. 9(b) has been used as a fixed-state map and Fig. 9(a) has been taken as initial and input image. In this experiment we have observed that the waves propagating from the external source can pass through the opening (see Fig. 9(c)). Experimentally it has been verified that if there are at least three cells active (i.e. not fixed), waves can pass through the opening.

The experiment has been repeated with the fixed-state from Fig. 10(a). Figure 10(b) shows that the waves propagate to the right on the inhomogeneous CNN arrays. The waves from the internal source are propagating in the opposite

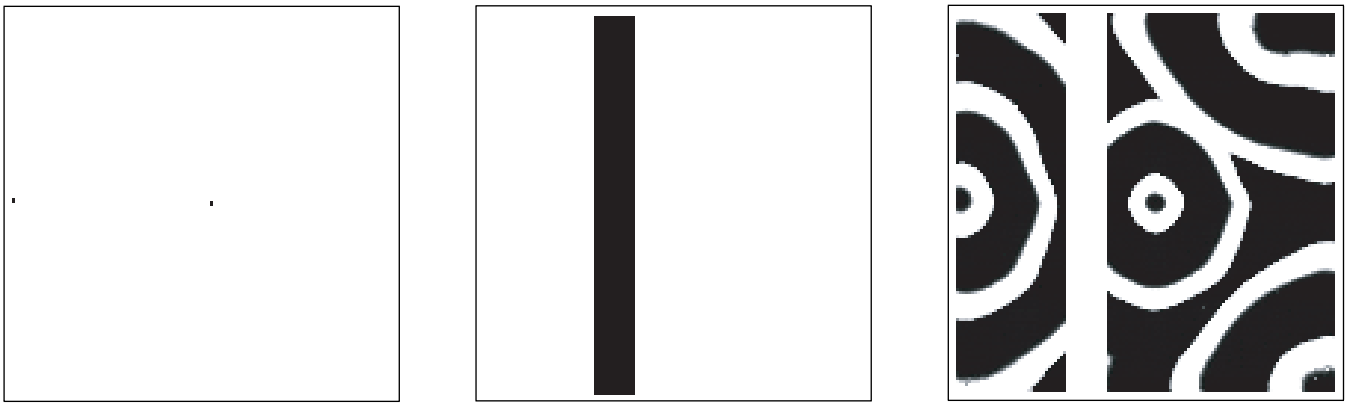

(a) (b) (c)

Fig. 8. (a) Image used as initial and input image. (b) Fixed-state map: The black regions correspond to state variable values that are fixed in time. (c) Propagation of autowaves on the CNN Universal Machine corresponding with fixed-state (a) using the same initial and input images as in (a).

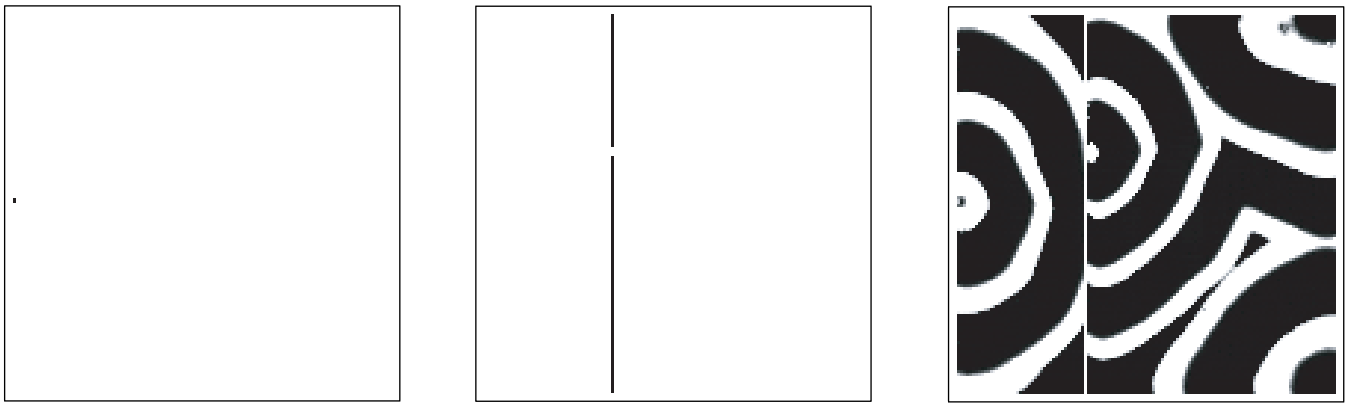

(a) (b) (c)

Fig. 9. (a) Image used as initial and input image. (b) Fixed-state map. (c) Propagation of autowaves on the CNN Universal Machine corresponding to fixed-state (b) using the same initial and input images as in (a).

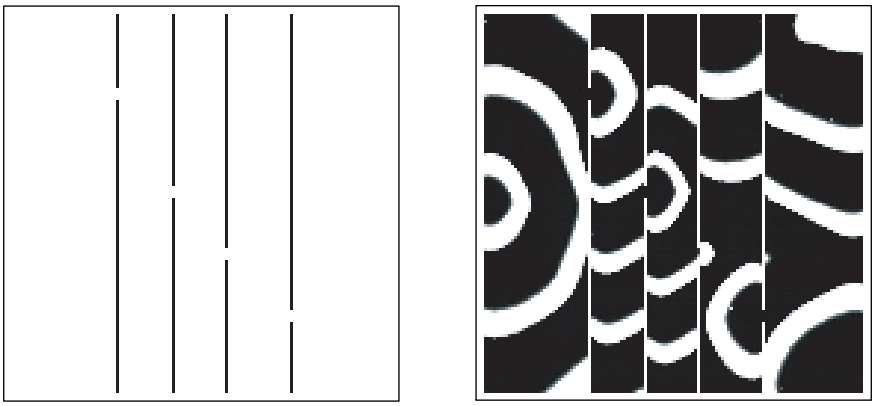

(a) (b)

Fig. 10. (b) Propagation of autowaves on the CNN Universal Machine corresponding to fixed-state using the same initial and input images of Fig. 9(a).

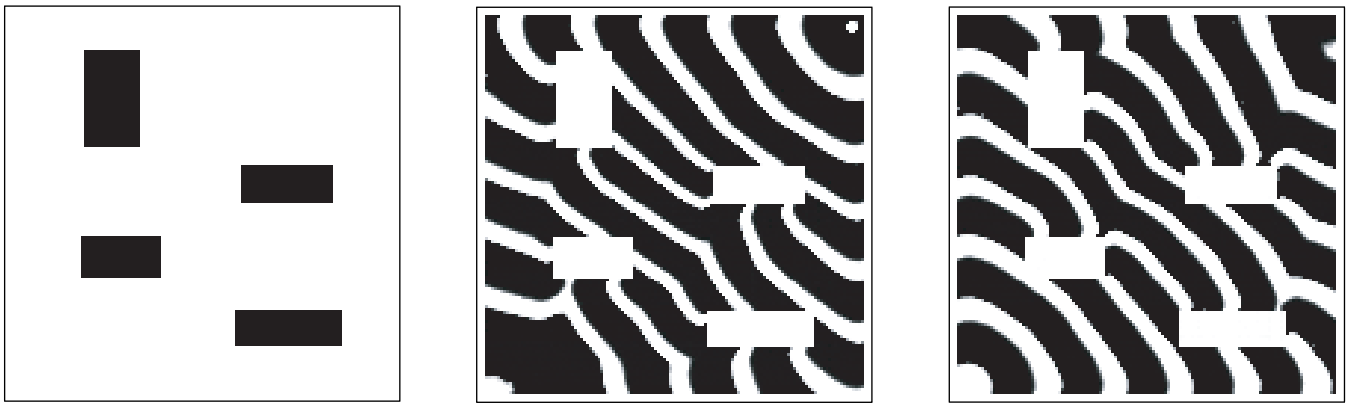

(a) (b) (c)

Fig. 11. (a) A fixed-state map. (b) and (c) Propagation of autowaves from the external sources which are located at top-right and bottom-left corners on the CNN corresponding to fixed-state (a), respectively. The waves continue to propagate around the frozen cells on the array.

direction. A competition between external and internal sources is taking place in the inhomogeneous network.

In the next experiment, using the fixed-state in Fig. 11(a), groups of inactive cells were defined on the network and an external source was located at the top-right corner. The propagation of autowaves from the top-right corner is shown in Fig. 11(b). The waves continue propagating around the frozen cells by the fixed-state map. The experiment has been repeated with a new external source located at the bottom-left corner. The propagation of autowaves is shown in Fig. 11(c) for this case.

5. Discussion

There can be two reasons for observing the presented spatial-temporal behavior on the ACE16k chip: (i) the order of the cells in the chip could be larger than one; (ii) the couplings to neighboring cells defined by the cloning template are different from zero, even when it is defined to be equal to zero in the templates via the digital interface. Using the fixed-state map of Fig. 12(a), 25 cells were randomly chosen in the chip and covered by frozen cells. In this way one can ensure that the coupling between the neighboring cells will not affect the cells dynamics. Figures 12(b)–12(d) show three consecutive snapshots for the templates 7 with Fig. 12(a) chosen as the fixed-state map. As seen in Figs. 12(b)–12(d) the cell states are changing in time. Hence, the order of the cells is larger than one. However, we assume that there exists a weak coupling between the cells, as synchronized behavior with the presented autowaves can result from an array of oscillating cells with weak coupling.

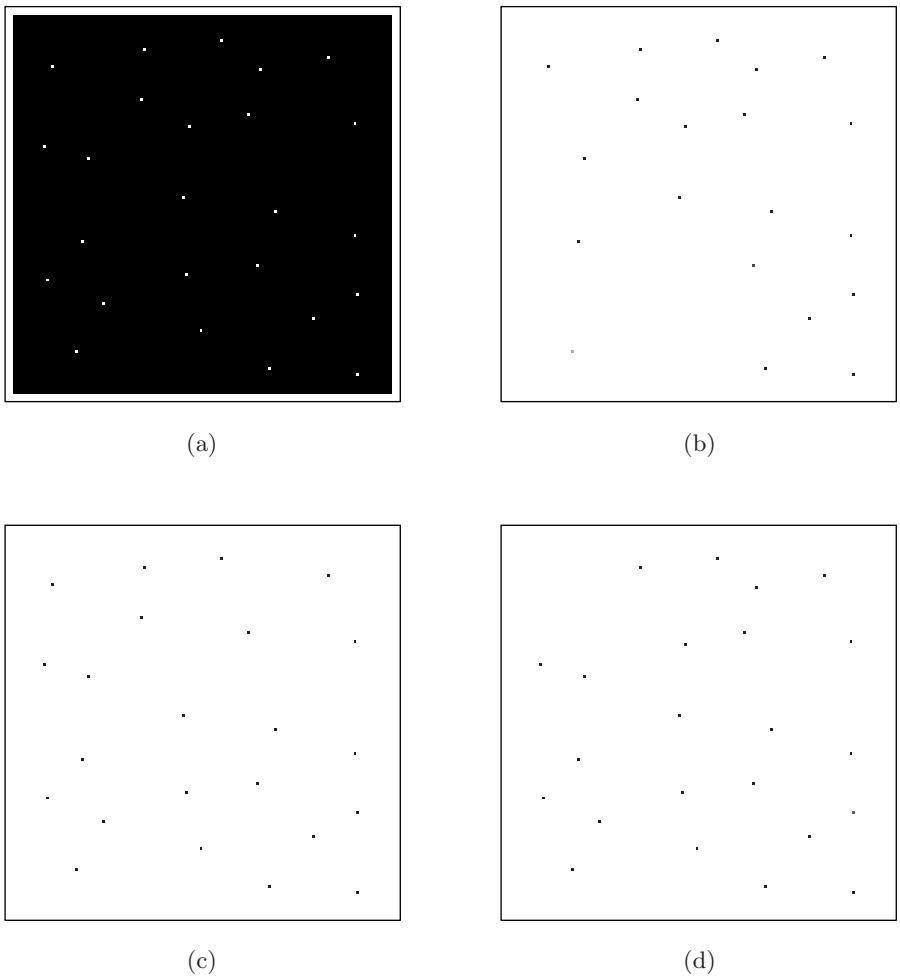

Fig. 12. (a) A fixed-map which is used to eliminate the coupling around the randomly chosen 25 cells. (b)–(d) Three consecutive snapshots for the template 7.

Acknowledgments

This research work was carried out at the ESAT laboratory and the Interdisciplinary Center of Neural Networks ICNN of the Katholieke Universiteit Leuven, in the framework of the Belgian Programme on Interuniversity Poles of Attraction, initiated by the Belgian State, Prime Minister's Office for Science, Technology and Culture (IUAP P4-02, IUAP P4-24, IUAP-V), the Concerted Action Project MEFISTO of the Flemish Community and the FWO project G.0080.01 *Collective Behavior and Optimization*: *an Interdisciplinary Approach*. Moreover, this work was supported by Istanbul Technical University.

References

Aladdin [2003] *Aladdin Professional*: *Hardware Manual*, Analogic Computers Ltd., Budapest, Version 3.0 edition.

Biey, M., Gilli, M. & Checco, P. [2002] "Complex dynamic phenomena in space-invariant cellular neural networks," *IEEE Trans. Circuits Syst.-I* **49**, 340–345.

Carmona, R., Jimenez-Garrido, F., Dominguez-Castro, R., Espejo, S., Roska, T., Rekecky, C., Petras, I. & Rodriguez-Vazquez, A. [2003] "A bio-inspired 2-layer mixed-signal flexible programmable chip for early vision," *IEEE Trans. Neural Networks* **14**, 1313–1336.

Chua, L. O., Hasler, M., Moschytz, G. & Neirynck, J. [1995] "Autonomous cellular neural networks: A unified paradigm for pattern formation and active wave propagation," *IEEE Trans. Circuits Syst.-I* **42**, 559–577.

Chua, L. O. [1998] *CNN*: *A Paradigm for Complexity* (World Scientific, Singapore).

Linan, G., Espejo, S., Dominguez-Castro, R. & Rodriguez-Vazquez, A. [2002] "Architectural and basic circuit considerations for a flexible 128×128 mixed-signal SIMD vision chip," *Anal. Integr. Circuits Sign. Process.* **33**, 179–190.

Manganaro, G., Arena, P. & Fortuna, L. [1999] *Cellular Neural Networks Chaos*, *Complexity and VLSI Processing* (Springer-Verlag, Berlin, Heidelberg).

Munuzuri, A. P., Munuzuri, V. P., Gesteria, M. G., Chua, L. O. & Villar, V. P. [1995] "Spatiotemporal structures in discretely-coupled arrays of nonlinear circuits: A review," *Int. J. Bifurcation and Chaos* **5**, 17–50.

Rodriguez-Vazquez, A., Linan-Cembrano, G., Carranza, L., Roca-Moreno, E., Carmona-Galan, R., Jimenez-Garrido, F., Dominguez-Castro, R. & Meana, S. E. [2004] "ACE16k: The third generation of mixed-signal SIMD-CNN ACE chips toward VSoCs," *IEEE Trans. Circuits Syst.-I* **51**, 851–863.

Roska, T. & Chua, L. O. [1993] "The CNN universal machine: An analogic array computer," *IEEE Trans. Circuits Syst.-I* **40**, 163–173.

Roska, T., Zarandy, A., Zold, S., Foldesy, P. & Szolgay, P. [1999] "The computational infrastructure of analogic CNN computing. I. the CNN-UM chip prototyping system," *IEEE Trans. Circuits Syst.-I* **46**, 261–268.

Yalçın, M. E., Suykens, J. A. K. & Vandewalle, J. [2004] "Experimental observation of autowaves on the ACE16k CNN chip," in *Proc. 8th IEEE Int. Workshop on Cellular Neural Networks and their Applications* (Budapest, Hungary), pp. 172–177.

Yalçın, M. E., Suykens, J. A. K. & Vandewalle, J. [2005] *Cellular Neural Networks*, *Multi-Scroll Chaos and Synchronization*, World Scientific Series on Nonlinear Science, Series A, Vol. 50 (World Scientific, Singapore).